Catal Lett (2012) 142:143–149
DOI 10.1007/s10562-011-0737-5

Theoretical Investigation of Ethanol Conversion to Ethylene over H–ZSM–5 and Transition Metals–Exchanged ZSM–5

Parisa Dumrongsakda · Vithaya Ruangpornvisuti

Received: 4 September 2011 / Accepted: 3 November 2011 / Published online: 15 November 2011

Abstract Reaction mechanisms of ethanol conversion to ethylene over H–ZSM–5, Cu–ZSM–5, Ag–ZSM–5, and Au–ZSM–5 catalysts were investigated using density functional theory calculations. Energetics, thermodynamic quantities, rate and equilibrium constants of ethanol conversion to ethylene were obtained using the B3LYP/LanL2DZ method. The catalytic abilities of these catalysts on the reaction rates of ethanol conversion to ethylene are in order: Au–ZSM–5 > > Ag–ZSM–5 > H–ZSM–5 > > Cu–ZSM–5.

Keywords H–ZSM–5 · Au(I), Ag(I) and Cu(I) exchanged H–ZSM–5 · Ethanol conversion to ethylene · DFT

1 Introduction

Production of light olefins from ethanol has many advantages. Zeolites have been widely used in the petrochemical industry as acid catalyzed processes and known as one of the most important heterogeneous catalysts [1–4]. Zeolites were widely studied for their acidic properties of Brønsted acid sites [5, 6] using several techniques [6–20]. Due to acidities of zeolites [21], the H–ZSM–5 was widely used as acid catalyst in the conversion of light alkanes to aromatics [22–29] and alkanes to alkenes [30].

The catalysts of exchanged cations on H–ZSM–5 known as bifunctional catalysts were used in many reactions [31–33]. The Zn/H–ZSM–5 [31], Co/H–ZSM–5 [32] Mo/H–ZSM–5 [33] were used in hydrocarbon conversion reactions. The Zn/H–ZSM–5 was used to increase propane conversion turnover rates, hydrogen formation rates, and selectivity to aromatics [31]. The Co/H–ZSM–5 was used for propane conversion to propene and to C_6–C_8 aromatics for dehydrogenation and dehydrocyclization of alkanes [32] and methylene reactions in Mo/H–ZSM–5 were investigated [33]. Many metal–exchanged ZSM–5 catalysts such as Cu–ZSM–5 [34–41] and Ag–ZSM–5 [42] were used in the elimination of nitrogen oxides (NO_X) emitted from vehicle exhausts and industrial sources.

In this work, we have theoretically investigated the reaction mechanisms of ethanol conversion to ethylene using metal–transition–ions–exchanged ZSM–5 (M–ZSM–5–type) catalysts in comparison with H–ZSM–5 catalyst. The M–ZSM–5–type catalysts where M = Cu(I), Ag(I) and Au(I) modeled as the 28T cluster have been theoretically employed and their reaction energies, thermodynamic properties, rate and equilibrium constants have been computed using the density functional theory calculations.

2 Computational Methods

The H–ZSM–5, M(I)–ZSM–5, where M(I) = Cu(I), Ag(I) and Au(I) were modeled as 28T clusters. The structure optimizations for these 28T–clusters and configurations of their interactions with ethanol reactant, ethylene

---

Electronic supplementary material The online version of this article (doi:10.1007/s10562-011-0737-5) contains supplementary material, which is available to authorized users.

P. Dumrongsakda
Center for Petroleum, Petrochemicals and Advanced Materials, Chulalongkorn University, Bangkok 10330, Thailand

V. Ruangpornvisuti (✉)
Department of Chemistry, Faculty of Science, Chulalongkorn University, Bangkok 10330, Thailand
e-mail: vithaya.r@chula.ac.th

product and their corresponding transition states were carried out using the density functional theory (DFT). The calculations were performed with GAUSSIAN 03 program [43] using Becke three–parameter exchange functional [44] with the Lee–Yang–Parr correlation functional [45] and the Los Alamos LanL2DZ split–valence basis set [46–48].

Fig. 1 The B3LYP/LanL2DZ–optimized structures of the cluster models for the **a** H–ZSM–5, **b** M(I)–ZSM–5 catalysts. The bond distances are in Å

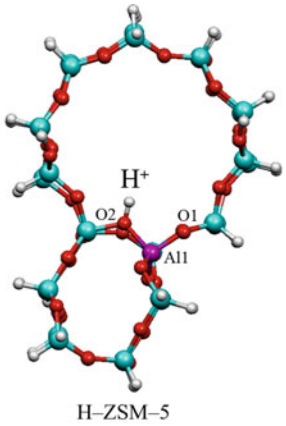

H–ZSM–5

(a)

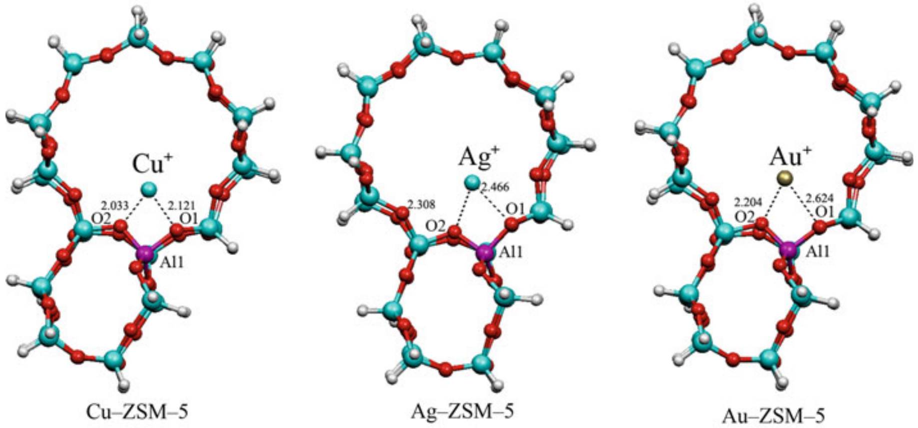

(b)

Fig. 2 The structure models employed in partial optimizations of the 28T clusters of the **a** H–ZSM–5, **b** M(I)–ZSM–5 where as their wireframe atoms are treated as frozen atoms and their ball-stick atoms are allowed to move

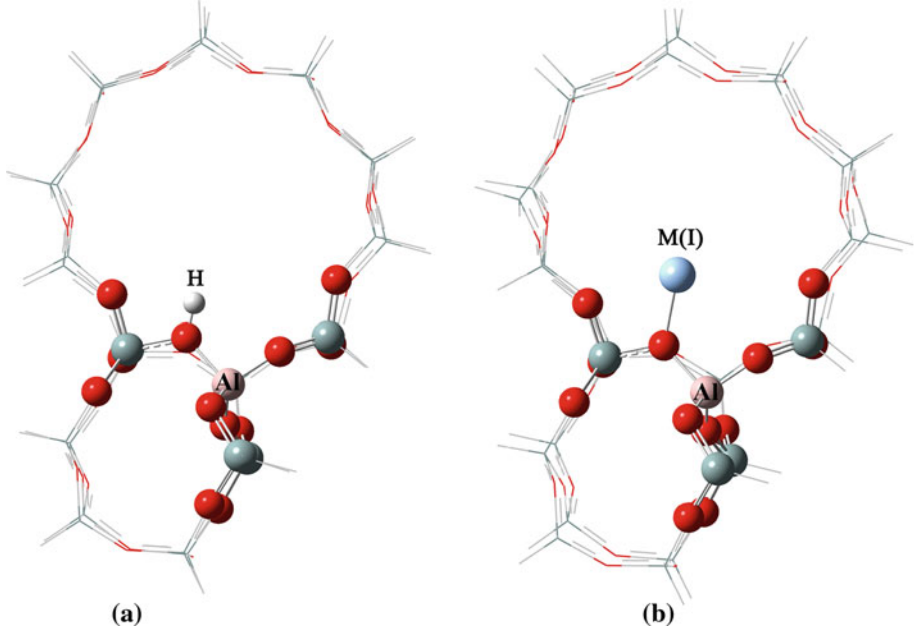

The zero point vibrational energy (ZPVE) corrections were derived from frequency calculations at the B3LYP/LanL2DZ level of theory.

2.1 Cluster Models for the H–ZSM–5 and M(I)–ZSM–5

The structure of 28T cluster of H–ZSM–5 zeolite was constructed from the idealized infinite ZSM–5 crystal lattice structure [49] and it was decorated as following treatment. The dangling bonds of 28T cluster of ZSM–5 were saturated with hydrogen atoms, its silicon atom located at the crystallographic position T12 was substituted by one aluminum atom and one hydrogen atom was bound to the oxygen atom which bridges between the T12–aluminum atom and its neighbor silicon atom as shown in Fig. 1a. The partial optimization of the 28T–cluster model of H–ZSM–5 which is composed of 27 silicon atoms and one aluminum atom (Si/Al = 27) and its formula is $H_{34}Si_{27}(HO)AlO_{38}$ was carried out with constrain of all atoms except all hydrogen atoms and 5T–cluster atoms ($(O_2Si–(OH)–Al(O–SiO_2)_3)$) containing the T12 site which is defined in Fig. 2a. The B3LYP/LanL2DZ–optimized structure of the H–ZSM–5 is shown in Fig. 1a.

The initial structures of M(I)–ZSM–5–type catalysts where M(I) = Cu(I), Ag(I), Au(I) were constructed by exchange of the hydrogen atom bound to the oxygen atom at the T12 site in the H–ZSM–5 with the monovalent metal ion, M(I) as shown in Fig. 2b.

The partial optimizations of the 28T–cluster model of M(I)–ZSM–5–type catalysts which are composed of 27 silicon atoms and one aluminum atoms (Si/Al = 27) and its formula is $H_{33}Si_{27}AlO_{39}$ M(I) were carried out with constrain of all atoms except all hydrogen atoms and 5T–cluster atoms as $(O_3Si)–(OM(I))–Al(O–SiO_2)$ $(O–SiO_3)_2$ which contains the T12 site as defined in Fig. 2b. The clusters for the H–ZSM–5 and the M(I)–ZSM–5 are denoted as the 28T (5T) cluster. The B3LYP/LanL2DZ–optimized structures of M(I)–ZSM–5 catalysts are shown in Fig. 1b.

2.2 Structure Optimization and Potential Energy Surface

The transition–state structures for ethanol conversion to ethylene on 28T (5T) cluster of the H–ZSM–5 and M(I)–ZSM–5 obtained at the B3LYP/LanL2DZ level of theory were located using the reaction coordinate method referred to the synchronous transit–guided quasi–newton (STQN) calculation [50]. The intrinsic reaction coordinate (IRC) method [51] was used to track minimum energy paths from transition structures to the corresponding minimum. All calculations were performed using GAUSSIAN 03 program [43].

2.3 Thermodynamic Properties and Formation Constants

The standard enthalpy ΔH^o_{298} and Gibbs free energy change ΔG^o_{298} of all studied reactions have been derived from the zero–point vibrational energy (ZPVE) [52] computed at the B3LYP/LanL2DZ level of theory. The rate constants $k(T)$ for conversion reactions of ethanol conversion to ethylene derived from the transition–state theory were computed from activation energy $\left(\Delta^{\ddagger}G\right)$ using Eq. (1) [52].

$$k(T) = \frac{k_{\mathrm{B}}T}{hc^o}\exp(-\Delta^{\ddagger}G^o/RT) \quad (1)$$

where the concentration factor of gases, c^o of unity is used, k_{B} is the Boltzmann's constant, h is Plank's

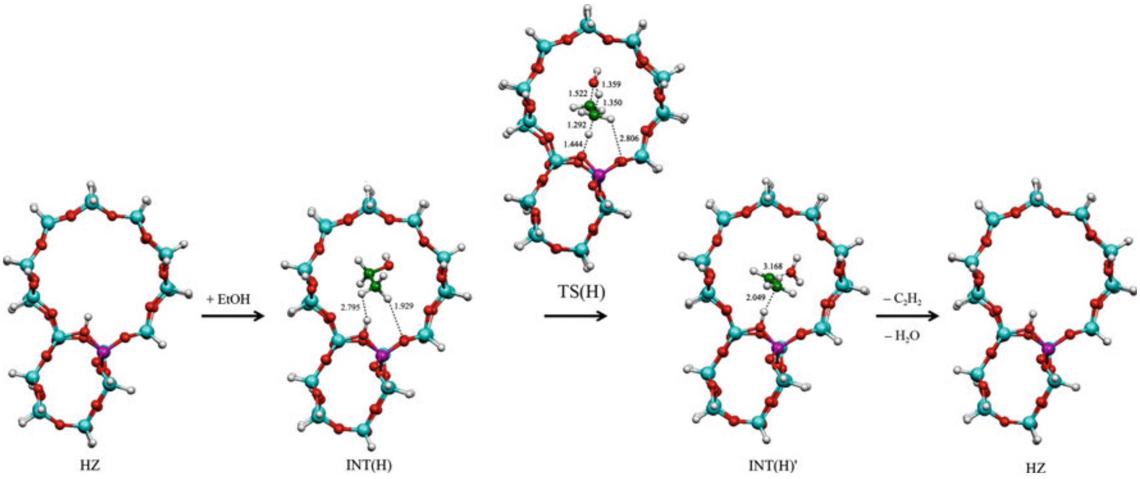

Fig. 3 Reaction mechanism for ethanol conversion to ethylene on the H–ZSM–5 catalyst, computed at the B3LYP/LanL2DZ level. The bond distances are in Å

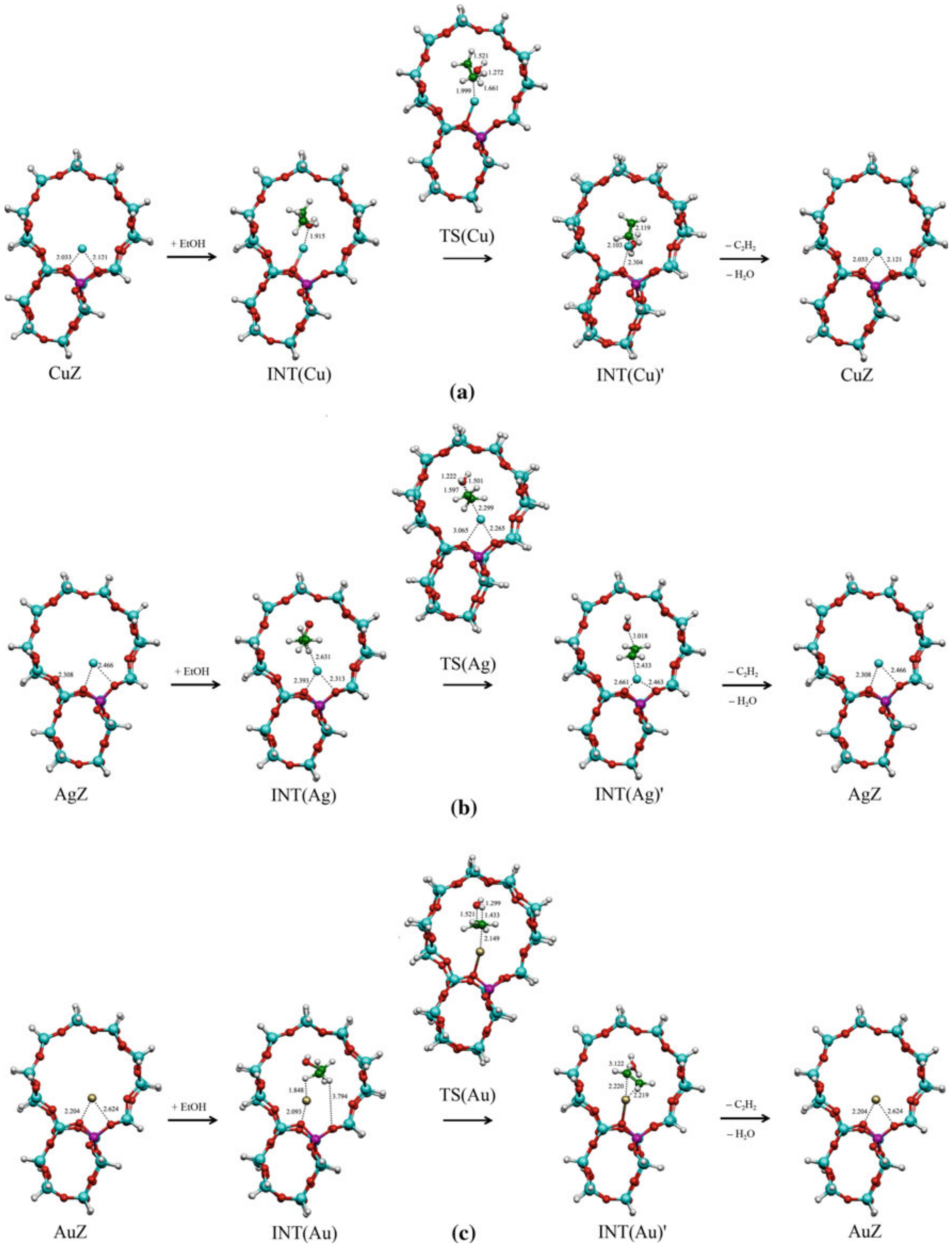

Fig. 4 Reaction mechanisms for ethanol conversion to ethylene on the **a** Cu–ZSM–5, **b** Ag–ZSM–5, **c** Au–ZSM–5 catalysts, computed at the B3LYP/LanL2DZ level. The bond distances are in Å

constant, T is the absolute temperature, and R is the gas constant. The equilibrium constant K at 298.15 K and 1 atm is computed using a thermodynamic equation $\Delta G^o = - RT \ln K$.

2.4 Rate Constant Ratio

A decision–making tool to evaluate for appropriate catalyst used in the certain reaction and the catalyst which results the high ratio of the rate constant to the lowest rate constant is probably good or appropriate. The rate constant ratio, $k_{\mathrm{I}}^{\mathrm{J}}$ is defined as a ratio of the rate constant of the certain reaction catalyzed by the J–catalyst ($k_{298}(\mathrm{J}-\mathrm{cat})$) to the lowest rate constant of the reaction catalyzed by the I–catalyst ($k_{298}(\mathrm{I}-\mathrm{cat})$), as shown in Eq. (2).

$$k_{\mathrm{I}}^{\mathrm{J}} = \frac{k_{298}(\mathrm{J}-\mathrm{cat})}{k_{298}(\mathrm{I}-\mathrm{cat})} \tag{2}$$

3 Results and Discussion

The B3LYP/LanL2DZ–optimized structures for the H–ZSM–5, Cu–ZSM–5 and Ag–ZSM–5 modeled as 28T cluster are shown in Fig. 1. It was found that mono–valent metal ions Cu(I), Ag(I), and Au(I) in the Cu–ZSM–5, Ag–ZSM–5, and Au–ZSM–5 are coordinated to two neighboring oxygen atoms which bond to the T12–aluminum atom as shown in Fig. 1b.

The optimized structures for the configurations of interactions between ethanol reactant, ethylene product and their corresponding transition state, and their reactions steps obtained by the partial optimizations at the B3LYP/LanL2DZ level are shown in Figs. 3, 4. All the B3LYP/LanL2DZ–optimized structures listed as atomic coordinates are shown in Table S1 (Supplementary material). The reaction mechanisms for ethanol conversion to ethylene on the H–ZSM–5 and M(I)–ZSM–5 catalysts are shown in Figs. 3, 4, respectively. The reaction mechanisms for ethanol conversion to ethylene whether over the H–ZSM–5 or M(I)–ZSM–5 are composed of three reaction steps namely (1) the adsorption of ethanol reactant on zeolite (2) the conversion of adsorption–states of ethanol to ethylene and (3) the desorption of the ethylene. The second reaction step for all the reaction was found to be the rate–determining step (RDS).

The selected geometrical parameters for configurations of interaction between reacting species and the H–ZSM–5 and M–ZSM–5 catalysts are listed in Table S2 (Supplementary material). Table S2 shows that the bond distances between cation and the nearest oxygen atom of ZSM–5 are O2–H = 0.977 Å, O2–Cu = 2.033 Å, O2–Ag = 2.308 Å and O2–Au = 2.204 Å, for the H–ZSM–5, Cu–ZSM–5, Ag–ZSM–5 and Au–ZSM–5 catalysts, respectively. The coordination numbers of the metal cation coordinated to

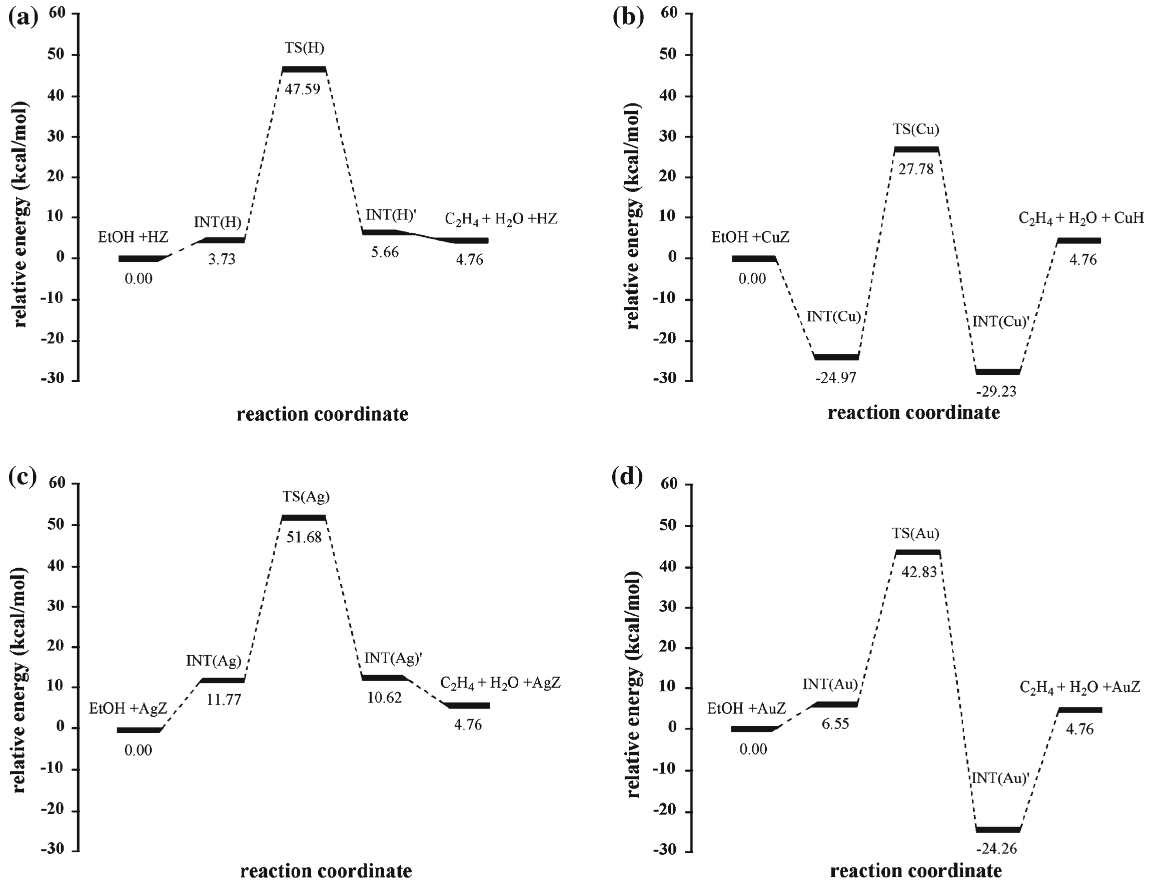

Fig. 5 Potential energy profiles for ethanol conversion to ethylene on the **a** H–ZSM–5, **b** Cu–ZSM–5, **c** Ag–ZSM–5, **d** Au–ZSM–5 catalysts

Table 1 Reaction energies, thermodynamic properties, rate constants and equilibrium constants for conversion reactions of ethanol to ethylene over the H–ZSM–5 and M(I)–ZSM–5 catalysts

Catalysts/Reactions[a]	$\Delta^{\ddagger}E^{a,b}$	$\Delta^{\ddagger}G^{a,b}$	k^{c}_{298}	k_{I}^{Jd}	ΔE^{a}	$\Delta H_{298}{}^{a}$	$\Delta G_{298}{}^{a}$	K_{298}
H–ZSM–5:								
EtOH + HZ → INT(H)	–	–	–		−7.98	−7.61	3.73	1.84×10^{-3}
INT(H) → TS(H) → INT(H)′	42.69	43.86	4.36×10^{-20}	3.28×10^{6}	2.28	3.11	1.93	3.82×10^{-2}
INT(H)′ → ZH + C_2H_4 + H_2O	–	–	–		19.09	19.46	−0.90	4.60×10^{0}
Cu–ZSM–5:								
EtOH + CuZ → INT(Cu)	–	–	–		−34.92	−34.19	−24.97	2.01×10^{18}
INT(Cu) → TS(Cu) → INT(Cu)′	52.33	52.75	1.33×10^{-26}	1.00×10^{0}	−4.73	−4.34	−4.26	1.34×10^{3}
INT(Cu)′ → CuZ + C_2H_4 + H_2O	–	–	–		53.04	53.49	34.00	1.20×10^{-25}
Ag–ZSM–5:								
EtOH + AgZ → INT(Ag)	–	–	–		−0.72	−0.51	11.14	6.68×10^{-9}
INT(Ag) → TS(Ag) → INT(Ag)′	40.45	40.51	1.25×10^{-17}	9.40×10^{8}	−1.73	−2.28	−0.54	2.50×10^{0}
INT(Ag)′ → AgZ + C_2H_4 + H_2O	–	–	–		15.85	17.76	−5.86	1.98×10^{4}
Au–ZSM–5:								
EtOH + AuZ → INT(Au)	–	–	–		−6.08	−6.27	−6.55	1.59×10^{-5}
INT(Au) → TS(Au) → INT(Au)′	34.57	36.29	1.56×10^{-14}	1.17×10^{12}	−29.71	−28.75	−30.81	3.85×10^{22}
INT(Au)′ → AuZ + C_2H_4 + H_2O	–	–	–		49.18	49.98	29.03	5.27×10^{-22}

[a] Computed at B3LYP/LanL2DZ level, in kcal mol^{-1}

[b] Activation energy

[c] In s^{-1}

[d] Defined in Eq. (2) as compared with the lowest rate constant of which the reaction is catalyzed by the Cu–ZSM–5

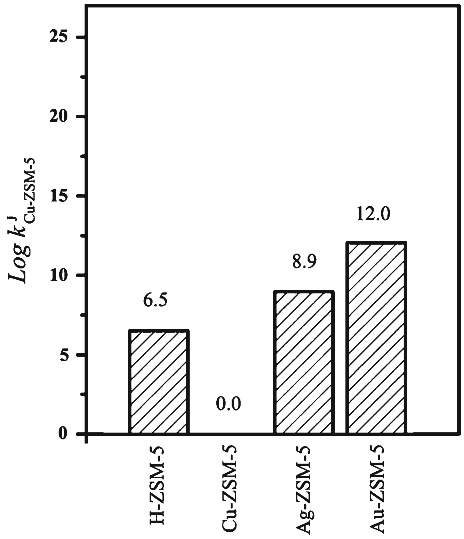

Fig. 6 Plot of the $Log\, k^{J}_{Cu-ZSM-5}$ against the modified ZSM–5 catalysts

the Cu–ZSM–5, Ag–ZSM–5 and Au–ZSM–5 catalysts in the vicinity of aluminum atoms are 2 as shown in Fig. 1.

The potential energy profiles for ethanol conversion to ethylene over the H–ZSM–5, Cu–ZSM–5, Ag–ZSM–5 and Au–ZSM–5 catalysts are shown in Fig. 5. The transition–states TS(H), TS(Cu), TS(Ag) and TS(Au) for the reaction catalyzed by the H–ZSM–5, Cu–ZSM–5, Ag–ZSM–5 and Au–ZSM–5 were proved by reaction paths of their intrinsic reaction coordinate (IRC) as shown in Figs. S1, S2, S3 and S4 in supplementary material, respectively.

Reaction energies, thermodynamic properties, rate and equilibrium constants for ethanol conversion to ethylene over the H–ZSM–5 and M(I)–ZSM–5 catalysts are shown in Table 1. Due to the RDS step, the reaction rates for ethanol conversion to ethylene on different catalysts are in order: Au–ZSM–5 ($\log\ k = -13.81$) > Ag–ZSM–5 ($\log\ k = -16.90$) > H–ZSM–5 ($\log\ k = -19.36$) > > Cu–ZSM–5 ($\log\ k = -25.88$). The magnitudes of equilibrium constants of the ethanol conversion to ethylene are in order: Au–ZSM–5 ($\log\ K = 22.59$) > > Cu–ZSM–5 ($\log K = 3.13$) ≈ Ag–ZSM–5 ($\log K = 0.40$) > H–ZSM–5 ($\log K = -1.42$). The activation energies due to the RDS step for ethanol conversion to ethylene over the H–ZSM–5, Cu–ZSM–5, Ag–ZSM–5 and Au–ZSM–5 catalysts as shown in Table 1 are 42.69, 52.33, 40.45, and 34.57 kcal/mol, respectively. Potential energy profiles for ethanol conversion to ethylene on the H–ZSM–5, Cu–ZSM–5, Ag–ZSM–5, and Au–ZSM–5 catalysts are shown in Fig. 5. The plot of the $Log\, k^{J}_{Cu-ZSM-5}$ against the modified ZSM–5 catalysts is shown in Fig. 6. It shows that the high activities of the noble metal–ions exchanged H–ZSM–5 catalysts on ethanol conversion to ethylene are found and in order: Au–ZSM–5 > Ag–ZSM–5.

4 Conclusions

Ethanol conversion to ethylene catalyzed by H–ZSM–5, Cu–ZSM–5, Ag–ZSM–5, and Au–ZSM–5 catalysts modeled as 28T–cluster was theoretically studied using the B3LYP/LanL2DZ method. The reaction rates for ethanol conversion to ethylene on different catalysts are in order: Au–ZSM–5 ($\log\ k = -13.81$) > Ag–ZSM–5 ($\log\ k = -16.90$) > H–ZSM–5 ($\log\ k = -19.36$) > > Cu–ZSM–5 ($\log\ k = -25.88$). The magnitudes of equilibrium constants of ethanol conversion to ethylene are in order: Au–ZSM–5 ($\log\ K = 22.59$) > > Cu–ZSM–5 ($\log\ K = 3.13$) $\approx$ Ag–ZSM–5 ($\log\ K = 0.40$) > H–ZSM–5 ($\log K = -1.42$). The catalytic activities of these catalysts on to the reaction rate are in order: Au–ZSM–5 > Ag–ZSM–5 > H–ZSM–5 > > Cu–ZSM–5.

Acknowledgments The National Nanotechnology Centre (NANOTEC), National Science and Technology Development Agency and the Thailand Research Fund (TRF) are gratefully acknowledged for the partial support of our MMCCRG laboratory, the Supramolecular Chemistry Research Unit (SCRU). We thank the Swiss Center for Scientific Computing, Manno, Switzerland for providing the program MOLEKEL 4.3.

References

1. Hölderich W, Hesse M, Näumann F (1988) Angew Chem Int Ed Engl 27:226
2. Corma A (1995) Chem Rev 95:559–614
3. Ghobarkar H, Schäf O, Guth U (1999) Prog Solid St Chem 27:29
4. Sen SE, Smith SM, Sullivan KA (1999) Tetrahedron 55:12657
5. Valyon J, Onyestyák G, Rees LVC (1998) J Phys Chem B 102:8994
6. Farneth WE, Gorte RJ (1995) Chem Rev 95:615
7. Yin F, Blumenfeld AL, Gruver V, Fripiat JJ (1997) J Phys Chem B 101:1824
8. Paukshtis EA, Malysheva LV, Stepanov VG (1998) React Kinet Catal Lett 65:145
9. Barthos R, Lónyi F, Onyestyák G, Valyon J (2000) J Phys Chem B 104:7311
10. Lónyi F, Valyon J (2001) Thermochim Acta 373:53
11. Lónyi F, Valyon J (2001) Microporous Mesoporous Mater 47:293
12. Boréave A, Auroux A, Guimon C (1997) Micropor Mater 11:275
13. Kao H–M, Grey CP (1996) J Phys Chem 100:5105
14. Jacobs WPJH, de Haan JW, van de Ven LJM, van Santen RA (1993) J Phys Chem 97:10394
15. Kapustin GI, Brueva TR (2001) Thermochim Acta 379:71
16. Katada N, Igi H, Kim J–H, Niwa M (1997) J Phys Chem B 101:5969
17. Brueva TR, Mishin IV, Kapustin GI (2001) Thermochim Acta 379:15
18. Parrillo DJ, Gorte RJ (1993) J Phys Chem 97:8786
19. Lee C, Parrillo DJ, Gorte RJ, Farneth WE (1996) J Am Chem Soc 118:3262
20. Zecchina A, Geobaldo F, Spoto G, Bordiga S, Ricchiardi G, Buzzoni R, Petrini G (1996) J Phys Chem 100:16584
21. Zhang X, Wang R, Yang X, Zhang F (2008) Microp Micropor Mesopo Mater 116:210
22. Kitagawa H, Sendoda Y, Ono Y (1986) J Catal 101:12
23. Shibata M, Kitagawa H, Sendoda Y, Ono Y (1986) Proceedings of the Seventh International Zeolite Conference, Elsevier, Tokyo, p. 717
24. Scurrell MS (1988) Appl Catal 41:89
25. Ono Y, Kanae K (1991) J Chem Soc Faraday Trans. 87:663
26. Shigeishi R, Garforth A, Harris I, Dwyer J (1991) J Catal 130:423
27. Guisnet M, Gnep NS, Aittaleb D, Doyemet JY (1992) Appl Catal 87:255
28. Guisnet M, Gnep NS, Alario F (1992) Appl Catal 89:1
29. Yoda E, Kondo JN, Domen K (2005) J Phys Chem B 109:1464
30. Xuebing L, Iglesia E (2008) J Catal 255:134
31. Biscardi JA, Meitzner GD, Iglesia E (1998) J Catal 179:192
32. Li W, Yu SY, Meitzner GD, Iglesia E (2001) J Phys Chem B 105:1176
33. Ding W, Li S, Meitzner GD, Iglesia E (2001) J Phys Chem B 105:506
34. Ma A–Z, Grünert W (1999) Chem Commun 71
35. Shelef M (1995) Chem Rev 95:209
36. Gómez SA, Campero A, Martinez–Hernández A, Fuentes GA (2000) Appl Catal A 197:157
37. Yahiro H, Iwamoto M (2001) Appl Catal A 222:163
38. Baik JH, Yim SD, Nam IS, Mok YS, Lee JH, Cho BK, Oh SH (2004) Top Catal 30–31:37
39. Rahkamaa–Tolonen K, Maunula T, Lomma M, Huuhtanen M, Keiski RL (2005) Catal Today 100:217
40. Yashnik SA, Ismagilov ZR, Anufrienko VF (2005) Catal Today 110:310
41. Berggrund M, Skoglundh M, Palmqvist AEC (2007) Top Catal 42/43:153
42. Shi C, Cheng M, Qu Z, Yang X, Bao X (2002) Appl Catal B 36:173
43. Frisch MJ, Trucks GW, Schlegel HB, Scuseria GE, Robb MA, Cheeseman JR, Montgomery Jr JA, Vreven T, Kudin KN, BurantJC,MillamJM, Iyengar SS, Tomasi J, BaroneV, Mennucci B, Cossi M, Scalmani G, Rega N, Petersson GA, Nakatsuji H, Hada M, Ehara M, Toyota K, Fukuda R, Hasegawa J, Ishida M, Nakajima T, Honda Y, Kitao O, Nakai H, KleneM, Li X, Knox JE, Hratchian HP, Cross JB, BakkenV,Adamo C, Jaramillo J, Gomperts R, Stratmann RE, Yazyev O, Austin AJ, Cammi R, Pomelli C, Ochterski JW,Ayala PY,Morokuma K,Voth, GA Salvador P, Dannenberg JJ, Zakrzewski VG, Dapprich S, Daniels AD, Strain MC, Farkas O, Malick DK, Rabuck AD, Raghavachari K, Foresman JB, Ortiz JV, Cui Q, Baboul AG, Clifford S, Cioslowski J, Stefanov BB, Liu G, Liashenko A, Piskorz P, Komaromi I, Martin RL, Fox DJ, Keith T, Al–Laham MA, Peng CY, Nanayakkara A, Challacombe M, Gill PMW, Johnson B, Chen W, Wong MW, Gonzalez C, Pople JA (2004) Gaussian 03, Revision D.02. Gaussian, Inc, Wallingford CT
44. Becke AD (1993) J Chem Phys 98:5648
45. Lee C, Yang W, Parr RG (1988) Phys Rev B 37:785
46. Hay PJ, Wadt WR (1985) J Chem Phys 82:270
47. Wadt WR, Hay PJ (1985) J Chem Phys 82:284
48. Hay PJ, Wadt WR (1985) J Chem Phys 82:299
49. Koningsveld HV, Bekkum HV, Jansen JC (1987) Acta Cryst B 43:127
50. Peng C, Ayala PY, Schlegel HB, Frisch MJ (1996) J Comp Chem 17:49
51. Gonzalez C, Schlegel HB (1989) J Chem Phys 90:2154
52. Ochterski JW (2000) Thermochemitry in gaussian. Gaussian, Pittsburgh